forests

MDPI

Article

Aboveground Biomass Allocation of Boreal Shrubs and Short-Stature Trees in Northwestern Canada

Linda Flade *, Christopher Hopkinson and Laura Chasmer

Department of Geography and Environment, University of Lethbridge, 4401 University Drive West, Lethbridge, AB T1K3M4, Canada; c.hopkinson@uleth.ca (C.H.); laura.chasmer@uleth.ca (L.C.)
* Correspondence: linda.flade@uleth.ca

Abstract: In this follow-on study on aboveground biomass of shrubs and short-stature trees, we provide plant component aboveground biomass (herein 'AGB') as well as plant component AGB allometric models for five common boreal shrub and four common boreal short-stature tree genera/species. The analyzed plant components consist of stem, branch, and leaf organs. We found similar ratios of component biomass to total AGB for stems, branches, and leaves amongst shrubs and deciduous tree genera/species across the southern Northwest Territories, while the evergreen *Picea* genus differed in the biomass allocation to aboveground plant organs compared to the deciduous genera/species. Shrub component AGB allometric models were derived using the three-dimensional variable volume as predictor, determined as the sum of line-intercept cover, upper foliage width, and maximum height above ground. Tree component AGB was modeled using the cross-sectional area of the stem diameter as predictor variable, measured at 0.30 m along the stem length. For shrub component AGB, we achieved better model fits for stem biomass (60.33 g $\leq$ RMSE $\leq$ 163.59 g; 0.651 $\leq R^2 \leq$ 0.885) compared to leaf biomass (12.62 g $\leq$ RMSE $\leq$ 35.04 g; 0.380 $\leq R^2 \leq$ 0.735), as has been reported by others. For short-stature trees, leaf biomass predictions resulted in similar model fits (18.21 g $\leq$ RMSE $\leq$ 70.0 g; 0.702 $\leq R^2 \leq$ 0.882) compared to branch biomass (6.88 g $\leq$ RMSE $\leq$ 45.08 g; 0.736 $\leq R^2 \leq$ 0.923) and only slightly better model fits for stem biomass (30.87 g $\leq$ RMSE $\leq$ 11.72 g; 0.887 $\leq R^2 \leq$ 0.960), which suggests that leaf AGB of short-stature trees (<4.5 m) can be more accurately predicted using cross-sectional area as opposed to diameter at breast height for tall-stature trees. Our multi-species shrub and short-stature tree allometric models showed promising results for predicting plant component AGB, which can be utilized for remote sensing applications where plant functional types cannot always be distinguished. This study provides critical information on plant AGB allocation as well as component AGB modeling, required for understanding boreal AGB and aboveground carbon pools within the dynamic and rapidly changing Taiga Plains and Taiga Shield ecozones. In addition, the structural information and component AGB equations are important for integrating shrubs and short-stature tree AGB into carbon accounting strategies in order to improve our understanding of the rapidly changing boreal ecosystem function.

Keywords: climate change; northern ecosystems; gross primary production; carbon cycling; permafrost; forest; peatland

Citation: Flade, L.; Hopkinson, C.; Chasmer, L. Aboveground Biomass Allocation of Boreal Shrubs and Short-Stature Trees in Northwestern Canada. *Forests* **2021**, *12*, 234. https://doi.org/10.3390/f12020234

Academic Editor: Brian Tobin
Received: 19 January 2021
Accepted: 16 February 2021
Published: 18 February 2021

1. Introduction

Boreal ecosystems of northwestern Canada store approximately 2.1% of the global terrestrial carbon (C) on 0.3% of the global land surface area [1]. Therefore, the global atmospheric climate-C cycle is tightly coupled to the changing C dynamics of northern boreal ecosystems [2]. For effective emissions targets and mitigation strategies, it is essential to reduce the high uncertainties of the C balance of unmanaged boreal ecosystems [2,3]. However, C accounting of unmanaged boreal ecosystems is challenging because these ecosystems are changing at unknown rates due to (1) the cumulative impacts of interacting climate-mediated and anthropogenic disturbances [4–8] and (2) the enhanced frequency,

intensity, duration, and timing of these disturbances. For example, in boreal ecosystems of northwestern Canada the vegetation structure and composition has changed significantly towards increased abundance of shrubs [9,10] and short-stature low productive or juvenile trees. This is in particular the case where ecosystems were set back to an early successional stage post wildland fire disturbance [11] or in the rapidly changing transition zones between elevated forests and adjacent peatlands due to permafrost thaw [8]. This in turn has significant effects on ecosystem function and ecosystem-atmosphere interactions at local to regional scales [8,11] as well as at national to global scales [12,13]. For example, prominent shrub and broadleaf tree growth in, e.g., post-fire vegetation succession is likely the explaining factor for returning production levels to an annual net C uptake within 10 to 15 years post burn (e.g., [12,14,15]). However, boreal shrubs and short-stature trees are not integrated into C accounting strategies. This is because of a lack of available spatially explicit structural and quantitative information on boreal shrub and short-stature tree species, as discussed in our related study [16]. Therefore, aboveground biomass (AGB) allocation data for shrubs and short-stature trees are necessary to better understand the contributions of different plant components to the standing stocks of AGB and aboveground C in this region, while plant component AGB allometric equations for shrubs and short-stature trees provide a means to improve modeling of AGB and aboveground C pools.

Consequently, the first objective of this paper was to describe and discuss the proportion of plant component AGB for boreal shrub and short-stature tree species. Plant components were separated into stems, branches, and leaves. The second objective was to provide allometric equations for estimating aboveground biomass of plant components of shrubs and short-stature trees. This paper is a follow-on study on shrub and short-stature tree total AGB allometric equations [16]. While in the previous study [16] we focused on total AGB allometric equations using 1D, 2D, and 3D predictor variables, in this study we analyze the AGB allocation to different plant components and provide plant component-specific allometric equations leveraging the same field data as described by Flade et al. [16]. The plant component data provided in this study is a crucial next step towards improved C pool partitioning required for improved C accounting strategies for unmanaged boreal ecosystems of northwestern Canada [3].

2. Materials and Methods

2.1. Study Area

Plant component AGB was derived from shrubs and short-stature trees growing in the mid-boreal Taiga Plains and high-boreal Taiga Shield ecoregions of the Northwest Territories (Figure 1). The climate in this region is characterized by cold mean annual air temperatures, ranging from −2.5 °C near Fort Simpson (Taiga Plains) to −3/−4 °C near Yellowknife (Taiga Shield). The area receives between 360 mm (Yellowknife) and 390 mm (Fort Simpson) cumulative annual precipitation. The genera and species sampled are *Alnus* spp., *Betula* spp., *Dasiphora fruticosa*, *Salix* spp., and *Shepherdia canadensis*, which represent common boreal shrub genera/species in this study area. Common boreal tree genera/species sampled are *Betula papyrifera*, *Picea glauca* and *mariana* (combined to *Picea* spp.), *Populus balsamifera*, and *Populus tremuloides* [17,18].

2.2. Plant Destructive Sampling

A total of 206 shrub and 105 tree individuals were measured and destructively sampled at 65 different peatland and forest sites. In order to capture the various stages of boreal ecosystem succession in our field data, field sampling locations were situated in late successional sites and in sites disturbed by wildland fire within the last 50 years. For a detailed field sampling plan, we refer to our previous study [16]. Trees were sampled within the last two weeks in July 2019, while shrubs were harvested during the late July/early August period of 2018 and 2019. Therefore, shrub foliage might show higher variability compared to tree foliage due to the potential influences of changes in phenology. Shrubs and short-stature trees were destructively sampled from the understory and open areas across

different height ranges determined in intervals of 0.5 m up to ≤4.5 m. A plant individual was selected for harvest when it was alive and mostly free of foliage disturbance/mortality and stem blemishes. Following measurements in situ [16], plants were clipped directly above the soil surface and stored in paper bags for further processing. Dead stems were not harvested. In the laboratory, harvested plants were air dried for up to 4 months and separated into stems, branches, and leaves. All plant components were oven dried at 60 °C for a minimum of 48 hrs. Constant mass was confirmed by weighing the largest plant individuals at multiple times post drying. Twigs and fruits were counted to the leaf component, while bark was included as part of the stem. For trees, branches were cut off directly at the stem. Shrubs did not develop distinctive branches and were separated into leave and stem components only. The total AGB for shrubs and trees was determined as dry weight (g) by weighing each plant component and summing the dry weight of all components per individual plant. In this study, we present measured plant component AGB as a percentage of the total AGB per plant genus/species.

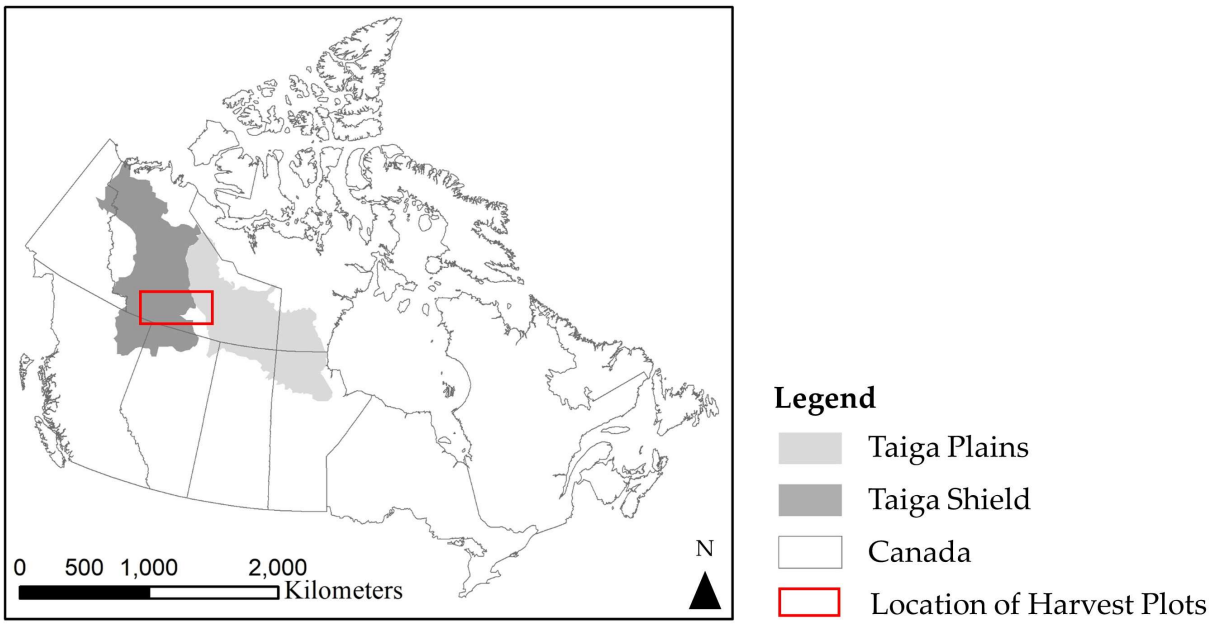

Figure 1. Area of harvested aboveground biomass of shrubs and trees, distributed across the sporadic to discontinuous permafrost zone of the Taiga Plains and Taiga Shield ecozones of boreal northwestern Canada.

2.3. In Situ Measurements and Plant Component Aboveground Biomass Allometric Equations

We derived AGB allometric equations for each plant component per plant genus/species as well as all shrub genera/species (multi-species shrubs) and tree genera/species (multi-species trees) combined. The methods follow the same procedures used to determine total AGB in [16]. The in situ structural measurements of harvested shrubs and trees used to determine the most accurate AGB predictions were volume for shrubs and cross-sectional area for trees [16]. Volume was derived by measuring the extent of the upper-most foliage layer perpendicular to the transect (herein 'width' [m]) and parallel to the transect (herein 'line-intercept cover' [m]) using a tape measure. The 3D shrub volume [m^3] was then calculated as

$$\text{Volume } [m^3] = \text{maximum height [m]} \times \text{line-intercept cover [m]} \times \text{width [m]}. \quad (1)$$

For short-stature trees, cross-sectional area [cm^2] was derived from the measured stem diameters. Stem diameters were measured at 0.30 m along the stem length starting from the average ground surface surrounding the tree [16].

Highest model fits were derived using iterative non-linear least squares regression (herein 'NLS') via a power function:

$$y = \beta x^{\alpha} + \varepsilon \quad (2)$$

where y is the dependent variable, x is the independent in situ variable (volume for shrubs and cross-sectional area for trees), α and β are the regression coefficients, and ε is an additive error term, as discussed by Flade et al. [16]. Because our AGB data showed uniform variances on arithmetic scales for most species as well as on logarithmic scales for all species, we did not apply weights to our models. In order to address potential heteroscedasticity in shrub and short-stature AGB data, we also developed ABG allometric equations using linear logarithmic regression with correction (herein 'LLRC'):

$$ln(y) = ln(\beta) + \alpha \times ln(x) + ln(\varepsilon) \quad (3)$$

$$y = \beta x^{\alpha} \times \varepsilon \quad (4)$$

$$\varepsilon = e^{(\frac{MSE}{2})} \quad (5)$$

where ε represents a multiplicative correction factor (CF) of the back-transformed arithmetic values, derived with MSE as the mean square error of the regression [16,19,20].

The modeled biomass results were evaluated using root mean square error (RMSE), coefficient of determination (R^2), and regression residual analysis. Residual analysis was performed using visual inspection of the relationships between dependent and independent variables. Regression coefficients are reported with standard errors.

3. Results and Discussion

3.1. Measured Plant Component AGB

The amounts of harvested individual plants per genus/species and descriptive statistics of measured plant component AGB are provided in Table 1. The percentages of the measured AGB per plant component is provided in Figure 2. We found similar plant AGB for leaves and stems for all five shrub genera/species, ranging from 15% (*Alnus* spp.) to 19% (*Betula* spp.) for leaves, and from 81% (*Betula* spp.) to 85% (*Alnus* spp.) for stems, respectively (Figure 2a). Similarly uniform was the measured plant component AGB for deciduous tree species, ranging from 10% (*Betula papyrifera*) to 16% (*Populus tremuloides*) leaf biomass, 12% (*Populus tremuloides*) to 17% (*Betula papyrifera*) branch biomass, and 72% (*Populus tremuloides*) to 77% (*Populus balsamifera*) stem biomass (Figure 2b). The measured plant component AGB of the evergreen *Picea* genus had lower stem biomass (49%) and higher branch (27%) and leaf (25%) biomass compared to the deciduous tree and shrub genera/species. This finding can be explained by the thick and often longer branches of the sampled *Picea* plants in comparison to the branches of short-stature deciduous tree species. We further found that the biomass of leaves and branches combined (52%) was approximately equal to the stem biomass (49%) of the *Picea* genus. Although biomass allocation changes with tree size and age (e.g. [21,22]), Petersson et al. [22] reported approximately 45% combined leave and branch biomass and 40% stem biomass (including bark) for 11 to 20 year old *Pinus sylvestris* stands in Sweden, while Johansson [23] derived a mean stem biomass proportion of 56% for 17 to 54 year old *Picea abies* stands growing on abandoned farmland in Sweden. In addition, we found that all five shrub genera/species had similar AGB allocations comparable to the three deciduous tree species.

Table 1. Descriptive statistic per plant genus/species and plant component (range of values in parentheses, average ± standard deviation).

Plant Genus/Species	No. of Samples	Maximum Height [m]	Total AGB [g]	AGB Stems [g]	AGB Branches [g]	AGB Leaves/ Needles [g]
Alnus spp.	33	[0.2; 3.2] 1.3 ± 0.7	[1.3; 2057.1] 311.4 ± 470.9	[0.6; 1856] 264.8 ± 401.8	-	[0.4; 289.7] 46.7 ± 68.0
Betula spp.	46	[0.2; 2.1] 1.1 ± 0.4	[4.0; 1154.1] 232.7 ± 261.1	[2.2; 1057.2] 188.2 ± 228.4	-	[1.3; 154.7] 44.5 ± 42.3
Dasiphora fruticosa	20	[0.2; 0.9] 0.6 ± 0.4	[5.1; 530.8] 117.6 ± 127.9	[3.6; 434.6] 96.2 ± 105.8	-	[1.5; 96.2] 21.4 ± 22.7
Salix spp.	79	[0.3; 2.8] 0.9 ± 0.5	[0.8; 1503.7] 143.3 ± 302.5	[0.4; 1381.4] 118.4 ± 261.1	-	[0.4; 284.8] 24.9 ± 47.0
Shepherdia canadensis	28	[0.3; 1.7] 0.8 ± 0.4	[7.1; 552.0] 121.5 ± 158.9	[5.7; 484.0] 99.5 ± 134.9	-	[1.1; 127.0] 22.0 ± 28.6
Betula papyrifera	15	[0.7, 3.4] 2.0 ± 0.8	[4.2; 596.2] 127.7 ± 162.2	[2.6; 444.9] 93.0 ± 122.4	[0.8; 95.7] 22.0 ± 26.1	[0.8; 55.6] 12.7 ± 14.8
Picea glauca	14	[0.4; 3.8] 1.8 ± 1.2	[10.5; 3021.8] 865.0 ± 992.4	[3.4; 1789.6] 426.1 ± 545.6	[1.2; 739.4] 212.5 ± 247.8	[5.9; 947.8] 226.4 ± 270.5
Picea mariana	15	[0.4; 3.6] 1.6 ± 0.9	[12.5; 2968.9] 668.5 ± 801.2	[4.3; 1269.6] 326.0 ± 412.2	[3.1; 1103.6] 195.2 ± 270.4	[5.1; 595.7] 157.1 ± 152.2
Populus balsamifera	31	[0.2; 4.2] 1.7 ± 1.1	[1.0; 380.9] 85.7 ± 103.3	[0.7; 294.9] 65.7 ± 81.3	[0.3; 53.1] 11.3 ± 13.7	[0.04; 47.0] 10.1 ± 11.1
Populus tremuloides	30	[0.4; 3.9] 1.8 ± 0.9	[1.1; 329.2] 67.8 ± 84.3	[0.5; 233.7] 50.2 ± 58.7	[0.04; 52.4] 8.6 ± 13.2	[0.2; 58.1] 10.9 ± 14.0

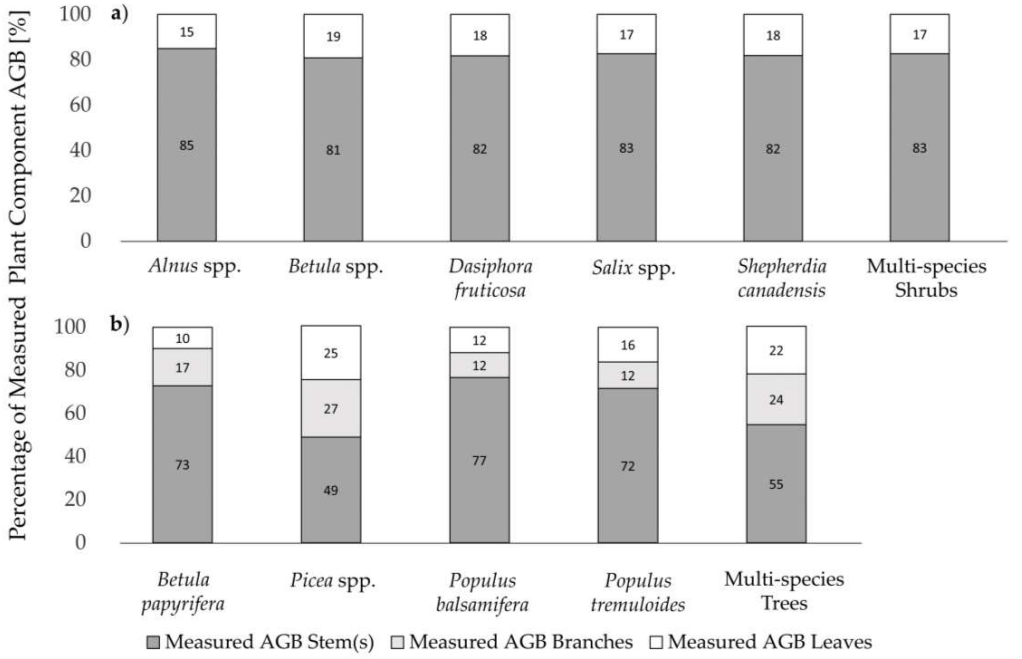

Figure 2. Measured aboveground biomass [%] per plant component for common boreal (**a**) shrub and (**b**) short-stature tree genera/species.

The variability of measured plant component AGB per shrub and short-stature tree genus/species is depicted in Figure 3a–g, respectively. From the five shrub genera/species sampled, *Alnus* spp. and *Betula* spp. were similar and showed greater variation compared to *Dasiphora fruticosa*, *Salix* spp., and *Shepherdia canadensis*. This differs from the findings of, e.g. He et al. [24], who found greatest structural differences between *Alnus* spp. and *Betula* spp. However, in our study *Betula* spp. showed greater differences in leaf biomass compared to all other genera/species, which is similar to the reported differences in total AGB of the *Betula* genus by the same authors [24]. In addition, we found similar structural growth forms of *Alnus* spp. and *Betula* spp. as reported by Lantz et al. [25] and Moffat et al. [26] for Arctic environments. *Alnus* spp. had stems growing in an outward radiating form, while both *Alnus* spp. and *Betula* spp. developed long shoots. However, *Salix* spp. was the dominant species in our study area compared to *Betula nana* dominance on lichen plots found in the Tuktoyaktuk coastland tundra [26]. Our study results showed further that *Salix* spp. had a lower median of stem biomass and more outliers compared to the other four genera/species. This might not only be due to greater structural variability of this genus, but also due to the larger sample amount (n = 79, Table 1), which increases the sampling of a greater range of structural variation. However, *Salix* spp. was the dominant genus at our field locations, and therefore, the larger sample amount represents the naturally dominant occurrence of *Salix* spp. in our study area. For deciduous short-stature tree genera/species, stem, branch, and leaf biomass (Figure 3d–g) showed similar variation, while *Picea* spp. had greater ranges, outliers, and medians for stem, branch, and leaf biomass, as previously described (Figure 2b). In addition, it needs to be mentioned that influences of phenological changes could be the reason for slightly greater shrub foliage AGB variation compared to deciduous tree foliage AGB variation, due to the measuring period of shrubs extending into early August (Figure 3c,g).

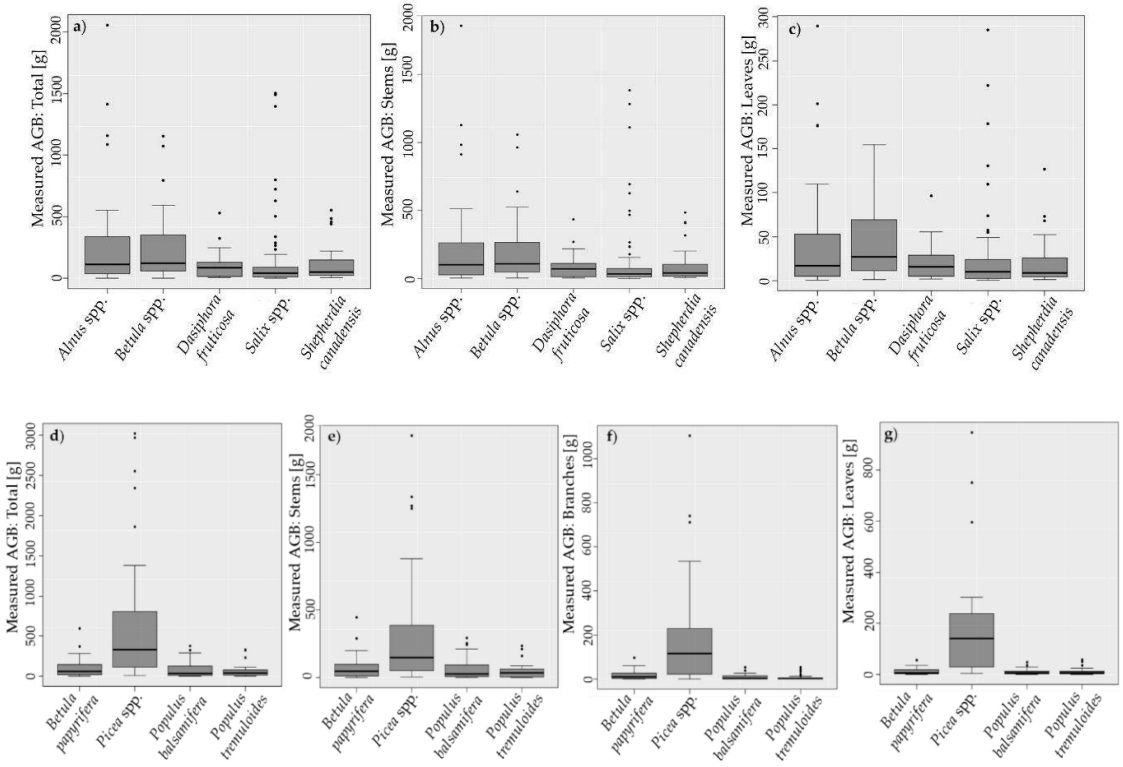

Figure 3. Boxplots of measured aboveground biomass [g] per plant component (total, stem, branch, and leaf aboveground biomass (AGB)) for common boreal (**a–c**) shrub and (**d–g**) short-stature tree genera/species. Points represent outliers of the distribution.

These findings suggest that short-stature deciduous tree genera/species may be combined with shrub genera/species as input into C allocation or terrestrial primary production models. However, model results might be improved when short-stature evergreen tree genera/species are analyzed separately, as already suggested by, e.g. Gower et al. [27], because these plant types differ in C budget processes, such as net primary production and C allocation [27–29], as well as percentage of plant component AGB. In addition, variations in plant traits, such as dry matter of leaves, adult plant height, leaf area, seed mass, leaf mass per area, and leaf nitrogen, vary among species as well as within species, in particular at local scales and in areas of low species richness (e.g., [30]). This suggests a need to additionally incorporate plant trait information in earth system models to improve understanding of the responses of plant communities, e.g., in ecosystem function and community assembly, to climate-mediated changes of environmental conditions [30]. The data used in this paper, does not provide the complete list of plant trait information, however, the plant component information might be useful as a first step towards improved earth system models in northern boreal environments.

3.2. Modeled Plant Component AGB and Allometric Equations

Regression coefficients and error statistics for the modeling of plant component AGB are provided for each genus/species as well as for multi-species shrubs (Table 2) and short-stature trees (Table 3). Because we found different AGB allocation of *Picea* spp., we also provided one combined component model for all deciduous tree species excluding *Picea* spp. (herein 'reduced hardwood tree model') (Table 3).

Table 2. Volume-based regression coefficient estimates with error statistics to be input into Equations (2)–(5) as appropriate to derive shrub component AGB.

		Model	LN (β)	β	SE (β)	α	SE (α)	CF	RMSE [g]	R^2
Alnus spp.	Stems	LLRC	5.104	164.6793		0.9474		1.2166	163.59	0.882
		NLS		146.3720	30.0176	1.0210	0.1021		137.23	0.885
	Leaves	LLRC	3.418	30.5083		0.7862		1.1792	35.04	0.735
		NLS		37.0392	8.5131	0.7805	0.1213		35.01	0.735
Betula spp.	Stems	LLRC	5.415	224.7525		0.8135		1.1766	137.05	0.651
		NLS		275.7010	28.2444	0.8980	0.1222		134.39	0.654
	Leaves	LLRC	3.977	53.3567		0.6370		1.2068	27.51	0.578
		NLS		64.8446	5.1663	0.6047	0.1019		27.48	0.579
Dasiphora fruticosa	Stems	LLRC	5.350	210.6083		0.7564		1.1608	60.72	0.672
		NLS		255.6900	31.3893	0.8490	0.2042		60.33	0.675
	Leaves	LLRC	3.714	41.0175		0.6228		1.1800	13.20	0.676
		ILS		55.9038	6.56778	0.8269	0.1911		12.62	0.691
Salix spp.	Stems	LLRC	5.161	174.3387		0.8857		1.1364	112.78	0.814
		NLS		210.9940	22.3109	0.8320	0.0588		111.90	0.817
	Leaves	LLRC	3.664	39.0171		0.7380		1.1767	33.75	0.519
		ILS		48.6847	5.6819	0.5734	0.0728		31.76	0.546
Shepherdia canadensis	Stems	LLRC	5.073	159.6526		0.7601		1.1018	62.16	0.789
		NLS		192.057	18.0495	0.6690	0.0849		60.68	0.801
	Leaves	LLRC	3.504	33.2482		0.6807		1.2342	23.74	0.380
		NLS		38.9539	5.84277	0.4535	0.1263		21.77	0.427
Multi-species Shrubs	Stems	LLRC	5.240	188.6701		0.8642		1.1842	123.31	0.795
		NLS		220.1460	12.7277	0.8170	0.0337		120.10	0.796
	Leaves	LLRC	3.692	40.1250		0.7151		1.2335	31.52	0.586
		NLS		50.4742	2.9920	0.5945	0.0393		30.12	0.600

Table 3. Regression coefficient estimates with error statistics based on cross-sectional area to be input into Equations (2)–(5) as appropriate to derive short-stature tree component AGB.

		Model	LN (β)	β	SE (β)	α	SE (α)	CF	RMSE [g]	R^2
Betula papyrifera	Stems	LLRC	3.970	52.9845		1.2370		1.0660	40.88	0.898
		NLS		41.4994	11.9728	1.5494	0.2193		36.63	0.913
	Branches	LLRC	2.634	13.9294		1.1440		1.0542	8.33	0.900
		NLS		12.7152	2.95996	1.2921	0.1826		8.08	0.905
	Leaves	LLRC	2.124	8.3645		1.0140		8.6012	70.00	0.882
		NLS		7.8627	2.1302	1.2143	0.2150		5.70	0.853
Picea spp.	Stems	LLRC	3.894	49.1069		1.0670		1.0782	170.97	0.928
		NLS		42.8437	11.9427	1.2201	0.1030		129.29	0.929
	Branches	LLRC	3.430	30.8766		1.0230		1.1129	94.07	0.892
		NLS		19.1842	6.6497	1.2866	0.1272		80.78	0.904
	Leaves	LLRC	3.821	45.6498		0.8059		1.1088	123.21	0.702
		NLS		42.2998	17.9815	0.9148	0.1635		119.89	0.704
Populus balsamifera	Stems	LLRC	3.805	44.9253		1.1320		1.1648	25.46	0.919
		NLS		47.3512	5.5776	1.3235	0.1053		22.43	0.924
	Branches	LLRC	1.773	5.8885		1.1140		1.4758	6.88	0.736
		NLS		7.6872	1.8698	1.2340	0.2211		6.83	0.737
	Leaves	LLRC	2.028	7.5989		1.0370		1.4577	5.81	0.832
		ILS		8.31954	1.1695	1.1007	0.1313		4.53	0.834
Populus tremuloides	Stems	LLRC	3.770	43.3801		1.0670		1.1627	13.64	0.950
		NLS		41.7058	3.0681	1.2658	0.0680		11.72	0.960
	Branches	LLRC	1.682	5.3763		1.0910		1.5380	6.18	0.816
		NLS		4.5910	1.0036	1.8127	0.1858		4.42	0.888
	Leaves	LLRC	2.255	9.5353		0.8919		1.1365	6.50	0.854
		NLS		8.07253	1.0364	1.4362	0.1149		4.11	0.917
Hardwood Trees	Stems	LLRC	3.830	46.0625		1.1220		1.1482	30.87	0.887
		NLS		41.4212	3.9694	1.4431	0.0807		26.48	0.904
	Branches	LLRC	1.927	6.8689		1.1270		1.4893	8.7	0.760
		NLS		6.4825	1.1607	1.5966	0.1475		8.00	0.789
	Leaves	LLRC	2.138	8.4825		0.9655		1.2434	5.57	0.826
		NLS		8.28683	0.8242	1.2225	0.0872		4.44	0.841
Multi-species Trees	Stems	LLRC	3.833	46.2009		1.1090		1.1296	80.19	0.939
		NLS		49.1790	5.0772	1.1712	0.0393		73.17	0.940
	Branches	LLRC	2.336	10.3398		1.2690		1.6568	51.61	0.919
		NLS		12.7920	2.2283	1.4315	0.0639		45.08	0.923
	Leaves	LLRC	2.584	13.2500		1.1070		1.5055	73.11	0.768
		NLS		20.2891	4.6584	1.1807	0.0872		67.96	0.767

Modeled total AGB that was derived by the sum of the single component AGB models was on average 0.13 g ± 1.67 g standard deviation (0.03% of modeled mean total AGB) higher for shrubs, and 1.88 g ± 1.09 g standard deviation (0.67%) higher for tress respectively, compared to the total AGB model results.

For shrub component AGB, we achieved better model fits for stem biomass (60.33 g ≤ RMSE ≤ 163.59 g; 0.651 ≤ R^2 ≤ 0.885) compared to leaf biomass (12.62 g ≤ RMSE ≤ 35.04 g; 0.380 ≤ R^2 ≤ 0.735) for each genus/species as well as for the general multi-species shrub model using the three-dimensional predictor variable volume. Higher prediction errors of leaf and branch biomass models vs. stem biomass models have been found as well by Lambert et al. [31]. However, except for *Shepherdia canadensis*, R^2 are above 0.5 for all other genera/species and multi-species shrubs (Table 2). For short-stature trees, leaf biomass predictions using cross-sectional area as the independent variable resulted in similar model fits (18.21 g ≤ RMSE ≤ 70.0 g; 0.702 ≤ R^2 ≤ 0.882) compared to branch biomass (6.88 g ≤ RMSE ≤ 45.08 g; 0.736 ≤ R^2 ≤ 0.923) and only slightly better model fits for stem biomass (30.87 g ≤ RMSE ≤ 11.72 g; 0.887 ≤ R^2 ≤ 0.960) for each genus/species as well as the general hardwood and multi-species tree models

(Table 3). This suggests that leaf biomass can be predicted using cross-sectional area as an independent variable for short-stature trees, leading to better results as the prediction of leaf biomass of tall-stature trees (diameter at breast height (DBH) > 9 cm) using DBH as an independent variable (e.g., [31,32]). Due to the different AGB allocation of *Picea* spp., we derived a reduced hardwood tree model including only the remaining hardwood tree species, as explained above. For this reduced hardwood tree model however, we did not receive better overall model fits ($0.760 \leq R^2 \leq 0.887$) compared to the full model that includes all tree genera/species ($0.767 \leq R^2 \leq 0.940$). In fact, model fits for stem and branch biomass were better for the full multi-species tree model. However, model fits for leaf biomass improved using the reduced hardwood tree model (Table 3).

The inspection of dependent vs. independent variable for the multi-species shrub and tree component models (Figure 4a,b) as well as the standardized residuals (Figure 4c,d) showed higher residuals of modeled leaf biomass compared to stem biomass for shrubs, while residuals were relatively homogeneous across all three modeled plant components for trees, as indicated by the goodness-of-fit metrics discussed above.

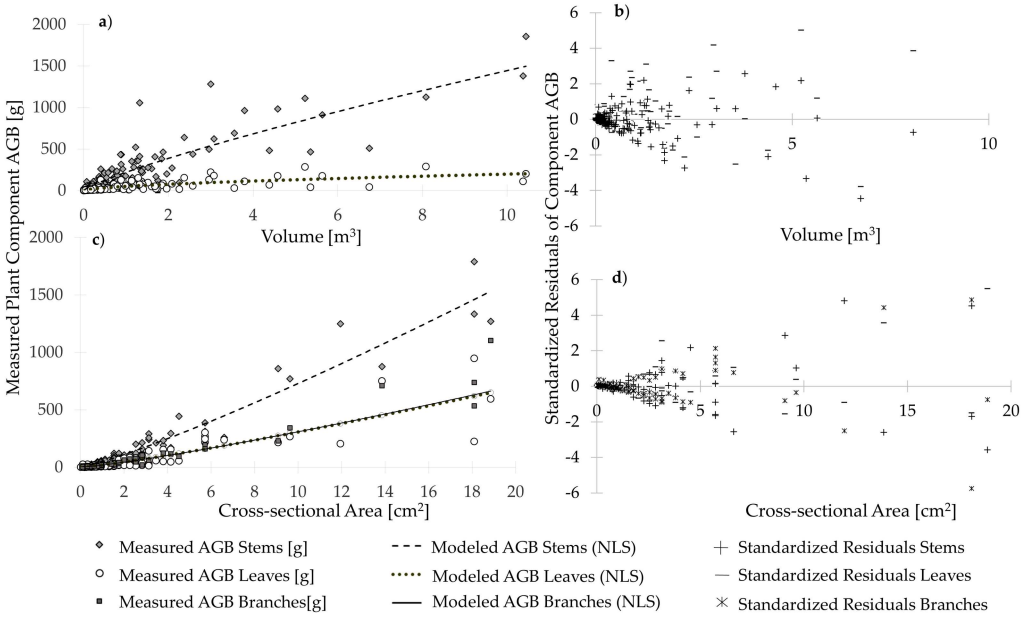

Figure 4. Model fits and standardized residuals per plant component for multi-species (**a**,**b**) shrub and (**c**,**d**) short-stature tree AGB. Shrub and tree component AGB was modeled via iterative nonlinear least-squares regression, using volume and cross-sectional area as the predictor variable, respectively.

For shrubs, the highest residuals were attributed to four shrub genera/species excluding *Sheperdia canadensis*, while the highest tree residuals corresponded to *Picea glauca* as well as *mariana*. Although this might imply that the multi-species tree component AGB models were mainly fit to *Picea* spp., we did not find higher residuals for smaller tree species in the multi-species component models. We achieved similar results with LLRC (not shown). This suggests that our multi-species models may have utility for using less invasive observation techniques (e.g., unmanned airborne vehicles or laser scanning) where vegetation species and type may be indeterminate. Furthermore, our genus/species-specific as well as multi-species models for predicting single plant component AGB may be well suited for scaling plant component and total AGB of shrubs and short-stature trees to the sporadic to discontinuous permafrost zones of the Taiga Plains and Taiga Shield ecozones of boreal northwestern Canada.

4. Conclusions

In this study we describe plant AGB allocation to leaf, branch, and stem components as well as plant component AGB allometric models for common boreal shrub and short-stature tree genera/species (<4.5 m height above ground) found in boreal northwestern Canada. We found similar AGB allocation to stems, branches, and leaves of shrubs and deciduous tree genera/species across our study region, while the sampled evergreen *Picea* genus differed in the AGB allocation to the aboveground plant components. Our plant component AGB allometric models showed better model fits for stem biomass compared to leaf biomass for shrubs. For short-stature trees, leaf biomass predictions resulted in similar model fits compared to branch biomass predictions with slightly better model fits for stem biomass predictions. In addition, our multi-species allometric models for shrubs and short-stature trees might be utilized for remote sensing techniques that do not allow to distinguish between plant functional types. This dataset and equations are a useful next step for integrating shrubs and short-stature tree AGB into C accounting strategies in order to improve our understanding of the rapidly changing boreal ecosystem function of forest and peatland ecosystems within the sporadic to discontinuous permafrost region. This provides an improved ability to develop full ecosystem models in the most climatically vulnerable and changing ecosystems found in the northern hemisphere.

Author Contributions: Conceptualization, L.F., C.H. and L.C.; methodology, L.F., C.H. and L.C.; validation, L.F. and L.C.; formal analysis, L.F.; investigation, L.F., C.H. and L.C.; resources, L.C. and C.H.; data curation, C.H.; writing—original draft preparation, L.F.; writing—review and editing, L.C., C.H., and L.F.; visualization, L.F.; supervision, L.C. and C.H.; project administration, L.C.; funding acquisition, L.C. and C.H. All authors have read and agreed to the published version of the manuscript.

Funding: This research was funded by the National Science and Engineering Research Council of Canada (NSERC)—Discovery Grants to Dr. Laura Chasmer and Dr. Christopher Hopkinson. Funding for field work has been provided by a start-up grant to Dr. Laura Chasmer from the University of Lethbridge. Further funding was provided by the Canadian Foundation of Innovation Award to Dr. Christopher Hopkinson.

Acknowledgments: Fieldwork was supported by the Government of the Northwest Territories—Tyler Rea and Ben Paulsen and the Dehcho Guardians program supported by William Quinton, Wilfrid Laurier University. For support in field data collection and biomass processing, the authors would like to thank Rachelle Shearing, Jesse Aspinall, Emily Jones, and Lavinia Haase from the University of Lethbridge, as well as Garrett Isiah with the Dehcho Guardian program. For provision of lab infrastructure (ovens) and expertise, we would like to thank Lawrence Flanagan from the University of Lethbridge. We also thank three anonymous reviewers for their careful reviews.

Conflicts of Interest: The authors declare no conflict of interest.

References

1. Vitt, D.H.; Halsey, L.A.; Bauer, I.E.; Campbell, C. Spatial and temporal trends in carbon storage of peatlands of continental western Canada through the Holocene. *Can. J. Earth Sci.* **2000**, *37*, 683–693. [CrossRef]
2. Kurz, W.A.; Shaw, C.H.; Boisvenue, C.; Stinson, G.; Metsaranta, J.; Leckie, D.; Dyk, A.; Smyth, C.; Neilson, E.T. Carbon in Canada's boreal forest—A synthesis. *Environ. Rev.* **2013**, *21*, 260–292. [CrossRef]
3. Bernier, P.; Kurz, W.A.; Lemprière, T.C.; Ste-Marie, C. *A Blueprint for Forest Carbon Science in Canada: 2012–2020*; Natural Resources Canada, Canadian Forest Service: Ottawa, ON, Canada, 2012; 52p.
4. Romero-Lankao, P.; Smith, J.B.; Davidson, D.J.; Diffenbaugh, N.S.; Kinney, P.L.; Kirshen, P.; Kovacs, P.; Villers Ruiz, L. North America. In *Climate Change 2014: Impacts, Adaption, and Vulnerability. Part B: Regional Aspects. Contribution of Working Group II to the Fifth Assessment Report of the Intergovernmental Panel on Climate Change*; Barros, V.R., Field, C.B., Dokken, D.J., Mastrandrea, M.D., Mach, K.J., Bilir, T.E., Chatterjee, M., Ebi, K.L., Estrada, Y.O., Genova, R.C., et al., Eds.; Cambridge University Press: Cambridge, UK; New York, NY, USA, 2014; pp. 1439–1498.
5. Dale, V.H.; Joyce, L.A.; McNulty, S.; Neilson, R.P.; Ayres, M.P.; Flannigan, M.D.; Hanson, P.J.; Irland, L.C.; Lugo, A.E.; Peterson, C.J.; et al. Climate Change and Forest Disturbances. *Bioscience* **2001**, *51*, 723. [CrossRef]
6. Quinton, W.L.; Hayashi, M.; Chasmer, L. Peatland Hydrology of Discontinuous Permafrost in the Northwest Territories: Overview and Synthesis. *Can. Water Resour. J.* **2009**, *34*, 311–328. [CrossRef]

7. Baltzer, J.; Veness, T.; Chasmer, L.; Sniderhan, A.E.; Quinton, W.L. Forests on Thawing Permafrost: Fragmentation, Edge Effects, and Net Forest Loss. *Glob. Chang. Biol.* **2014**, *20*, 824–834. [CrossRef] [PubMed]
8. Chasmer, L.; Hopkinson, C. Threshold Loss of Discontinuous Permafrost and Landscape Evolution. *Glob. Chang. Biol.* **2017**, *23*, 2672–2686. [CrossRef]
9. Myers-Smith, I.H.; Forbes, B.C.; Wilmking, M.; Hallinger, M.; Lantz, T.C.; Blok, D.; Tape, K.D.; Macias-Fauria, M.; Sass-Klaassen, U.; Lévesque, E.; et al. Shrub expansion in tundra ecosystems: Dynamics, impacts and research priorities. *Environ. Res. Lett.* **2011**, *6*, 045509. [CrossRef]
10. Myers-Smith, I.H.; Kerby, J.T.; Phoenix, G.K.; Bjerke, J.W.; Epstein, H.E.; Assmann, J.J.; John, C.; Andreu-Hayles, L.; Angers-Blondin, S.; Beck, P.S.A.; et al. Complexity revealed in the greening of the Arctic. *Nat. Clim. Chang.* **2020**, *10*, 106–117. [CrossRef]
11. Helbig, M.; Chasmer, L.E.; Kljun, N.C.; Quinton, W.L.; Treat, C.C.; Sonnentag, O. The positive net radiative greenhouse gas forcing of increasing methane emissions from a thawing boreal forest-wetland landscape. *Glob. Chang. Biol.* **2017**, *23*, 2413–2427. [CrossRef]
12. Goulden, M.L.; Mcmillan, A.M.S.; Winston, G.C.; Rocha, A.V.; Manies, K.L.; Harden, J.W.; Bond-Lamberty, B.P. Patterns of NPP, GPP, respiration, and NEP during boreal forest succession. *Glob. Chang. Biol.* **2011**, *17*, 855–871. [CrossRef]
13. Goetz, S.J.; MacK, M.C.; Gurney, K.R.; Randerson, J.T.; Houghton, R.A. Ecosystem responses to recent climate change and fire disturbance at northern high latitudes: Observations and model results contrasting northern Eurasia and North America. *Environ. Res. Lett.* **2007**, *2*, 045031. [CrossRef]
14. Amiro, B.; Orchansky, A.; Barr, A.; Black, T.; Chambers, S.; Iii, F.C.; Goulden, M.; Litvak, M.; Liu, H.; McCaughey, J.; et al. The effect of post-fire stand age on the boreal forest energy balance. *Agric. For. Meteorol.* **2006**, *140*, 41–50. [CrossRef]
15. Beck, P.S.A.; Goetz, S.J. Satellite observations of high northern latitude vegetation productivity changes between 1982 and 2008: Ecological variability and regional differences. *Environ. Res. Lett.* **2011**, *6*, 045501. [CrossRef]
16. Flade, L.; Hopkinson, C.; Chasmer, L. Allometric equations for shrub and short-stature tree aboveground biomass within boreal ecosystems of northwestern Canada. *Forests* **2020**, *11*, 1207. [CrossRef]
17. Ecosystem Classification Group. *Ecological Regions of the Northwest. Territories—Taiga Plains. Department of Environment and Natural Resources*; Government of the Northwest Territories: Yellowknife, NT, Canada, 2007.
18. Ecosystem Classification Group. *Ecological Regions of the Northwest. Territories—Taiga Shield. Department of Environment and Natural Resources*; Government of the Northwest Territories: Yellowknife, NT, Canada, 2008.
19. Baskerville, G.L. Use of logarithmic regression in the examination of plant biomass. *Can. J. For.* **1972**, *2*, 49–53.
20. Mascaro, J.; Labs, P.; Litton, C.M.; Schnitzer, S. Minimizing Bias in Biomass Allometry: Model Selection and Log—Transformation of Data. *Biotropica* **2011**, *43*, 649–653. [CrossRef]
21. Konôpka, B.; Pajtík, J.; Moravčík, M.; Lukac, M. Biomass partitioning and growth efficiency in four naturally regenerated forest tree species. *Basic Appl. Ecol.* **2010**, *11*, 234–243. [CrossRef]
22. Petersson, H.; Holm, S.; Ståhl, G.; Alger, D.; Fridman, J.; Lehtonen, A.; Lundström, A.; Mäkipää, R. Individual tree biomass equations or biomass expansion factors for assessment of carbon stock changes in living biomass—A comparative study. *For. Ecol. Manag.* **2012**, *270*, 78–84. [CrossRef]
23. Johansson, T. Biomass production of Norway spruce (Picea abies (L.) Karst) growing on abandoned farmland. *Silva. Fenn.* **1999**, *33*, 261–280. [CrossRef]
24. He, A.; McDermid, G.J.; Rahman, M.M.; Strack, M.; Saraswati, S.; Xu, B. Developing allometric equations for estimating shrub biomass in a boreal fen. *Forests* **2018**, *9*, 569. [CrossRef]
25. Lantz, T.C.; Marsh, P.; Kokelj, S. Recent Shrub Proliferation in the Mackenzie Delta Uplands and Microclimatic Implications. *Ecosystems* **2013**, *16*, 47–59. [CrossRef]
26. Moffat, N.D.; Lantz, T.C.; Fraser, R.H.; Olthof, I. Recent vegetation change (1980–2013) in the tundra ecosystems of the Tuktoyaktuk Coastlands, NWT, Canada. *Arct. Antarct. Alp. Res.* **2016**, *48*, 581–597. [CrossRef]
27. Gower, S.T.; Vogel, J.G.; Norman, M.; Kucharik, C.J.; Steele, S.J. Carbon distribution and aboveground net primary production in aspen, jack pine, and black spruce stands in Saskatchewan and Manitoba, Canada. *J. Geophys. Res.* **1997**, *29*. [CrossRef]
28. Bonan, G. Ecosystems. In *Ecological Climatology*; Cambridge University Press: Cambridge, UK, 2016; pp. 328–357. [CrossRef]
29. Baldocchi, D.; Vogel, C. Energy and CO2 flux densities above and below a temperate broad-leaved forest and a boreal pine forest. *Tree Physiol.* **1996**, *16*, 5–16. [CrossRef]
30. Thomas, H.J.D.; Bjorkman, A.D.; Myers-Smith, I.H.; Elmendorf, S.C.; Kattge, J.; Diaz, S.; Vellend, M.; Blok, D.; Cornelissen, J.H.C.; Forbes, B.C.; et al. Global plant trait relationships extend to the climatic extremes of the tundra biome. *Nat. Commun.* **2020**, *11*. [CrossRef]

31. Lambert, M.-C.; Ung, C.-H.; Raulier, F. Canadian national tree aboveground biomass equations. *Can. J. For. Res.* **2005**, *35*, 1996–2018. [CrossRef]
32. Ung, C.H.; Bernier, P.; Guo, X.J. Canadian national biomass equations: New parameter estimates that include British Columbia data. *Can. J. For. Res.* **2008**, *38*, 1123–1132. [CrossRef]